BBA - Molecular Basis of Disease 1865 (2019) 2333–2341

Contents lists available at ScienceDirect

BBA - Molecular Basis of Disease

journal homepage: www.elsevier.com/locate/bbadis

IDH2 deficiency exacerbates acetaminophen hepatotoxicity in mice via mitochondrial dysfunction-induced apoptosis

Hyunjin Kim[a], Jin Hyup Lee[b], Jeen-Woo Park[a,*]

[a] School of Life Sciences and Biotechnology, BK21 Plus KNU Creative BioResearch Group, College of Natural Sciences, Kyungpook National University, Taegu, Republic of Korea

[b] Department of Food and Biotechnology, Korea University, Sejong, Republic of Korea

ARTICLE INFO

Keywords:
IDH2
Acetaminophen
ER stress
Mitochondrial dysfunction
Reactive oxygen species

ABSTRACT

Acetaminophen (APAP)-induced hepatotoxicity is a major factor in liver failure and its toxicity is associated with the generation of reactive oxygen species (ROS), decreased levels of reduced glutathione (GSH) and overall oxidative stress. Mitochondrial $NADP^+$-dependent isocitrate dehydrogenase (IDH2) was demonstrated as an essential enzyme for mitochondria to maintain their antioxidant system by generating NADPH, which is an essential reducing equivalent for GSH turnover in mitochondria. Here, we investigated the role of IDH2 in APAP-induced liver injury with IDH2 deficient ($idh2^{-/-}$) mice. Hepatotoxicity was promoted through apoptotic cell death following APAP administration in IDH2 deficient hepatocytes compared to that in wild-type hepatocytes. Apoptosis was found to result from the induction of ER stress and mitochondrial dysfunction as shown by the blocking the effect of phenylbutyrate and Mdivi1, respectively. In addition, mito-TEMPO, a scavenger of mitochondrial ROS, was seen to ameliorate APAP-induced hepatotoxicity in $idh2^{-/-}$ mice. In conclusion, IDH2 deficiency leads to a fundamental shortage of GSH that increases susceptibility to ROS generation and oxidative stress. This leads to excessive mitochondrial dysfunction and ER stress induction in response to APAP administration. Our study provides further evidence that IDH2 has a protective role against APAP-induced liver injury and emphasizes the importance of the elaborate linkages and functions of the antioxidant system in liver health.

1. Introduction

Acetaminophen (APAP) is the most widely used painkiller and is generally known for its safety and efficacy. However, APAP overdose can cause toxicity in the liver that leads to liver failure. Liver injury and acute liver failure induced by drugs remains a considerable problem in Western societies [1]. APAP-induced toxicity accounts for at least 42% of acute liver failure cases at tertiary hospitals and one third of the deaths in the U.S. each year [2]. APAP-induced hepatotoxicity is distinguishable by its substantial oxidative stress generation [3]. When APAP is bioactivated, reactive oxygen species (ROS) are generated and the metabolite depletes glutathione (GSH) [4–6]. ROS are generated as byproducts of aerobic metabolism, defense mechanisms against pathogens and various types of stress. ROS oxidizes components of cells such as proteins, lipids, and nucleic acids and this oxidation eventually causes harm to cells [7].

To protect against oxidative stress, cells possess antioxidant defense systems. These systems, which include catalase, superoxide dismutase, glutaredoxin, and peroxiredoxin, require GSH and NADPH as reducing agents [10]. Thus, repletion of GSH reduces APAP-induced hepatotoxicity [11]. Evidence suggests that mitochondria are a major site of ROS formation during APAP overdose, which leads to severe liver injury [8,9]. The mitochondrial $NADP^+$-dependent isocitrate dehydrogenase (IDH2) catalyzes isocitrate to α-ketoglutarate, producing NADPH, which is a fundamental cofactor for regeneration of GSH in the thioredoxin system [12]. Therefore, IDH2 regulates the mitochondrial redox status and decreases oxidative stress in cells [13].

Herein, we hypothesize that retardation of GSH reduction in an IDH2 deficient mouse model increases susceptibility to APAP hepatotoxicity. Previously, we studied the role of IDH2 in carcinogenesis [14], neurodegenerative disease [15], colitis [16] and LPS-induced inflammation [17]. In the present study, we investigate the effects of IDH2 deficiency in APAP-induced liver injury and the mechanisms involved in the associated cell death pathways.

* Corresponding author.
E-mail address: parkjw@knu.ac.kr (J.-W. Park).

https://doi.org/10.1016/j.bbadis.2019.05.012
Received 21 January 2019; Received in revised form 15 May 2019; Accepted 17 May 2019
Available online 20 May 2019

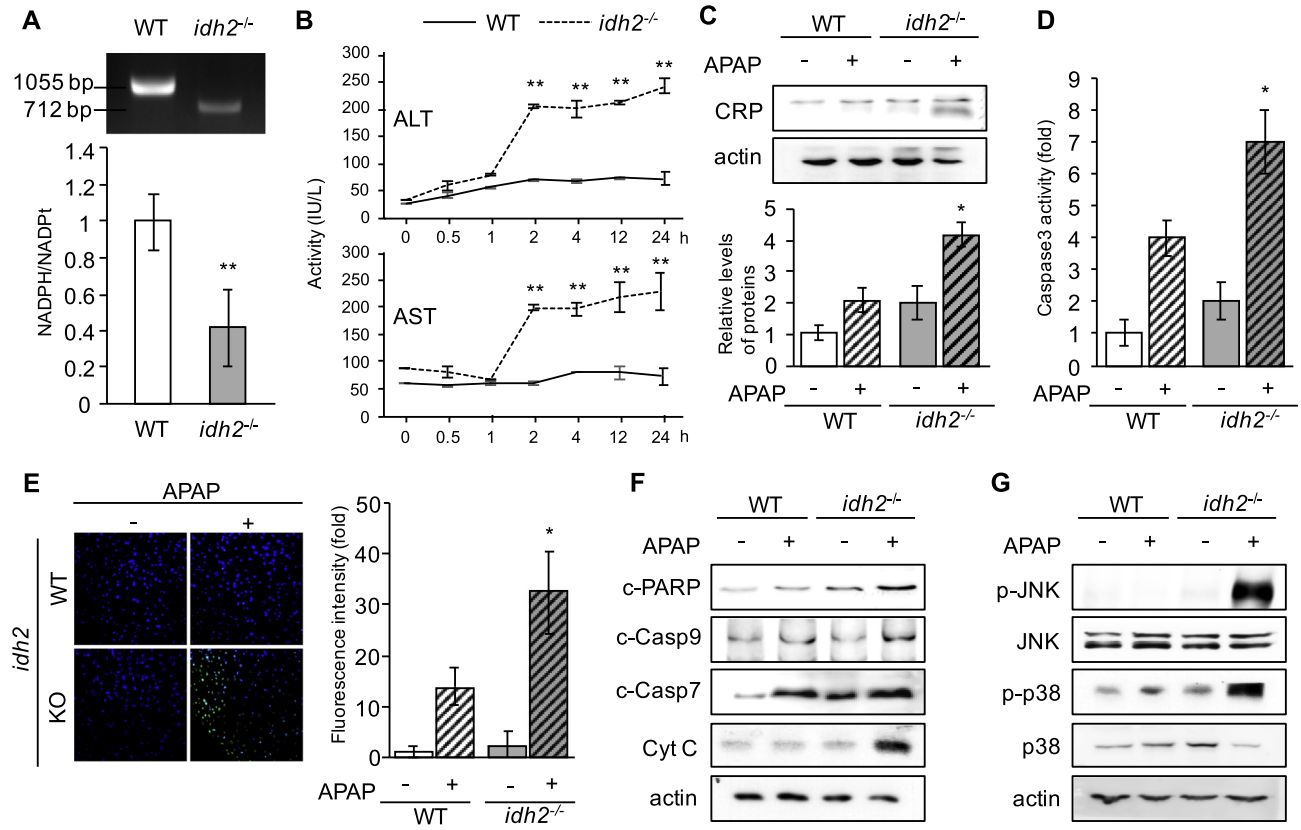

Fig. 1. Knockout of IDH2 in C57BL/6 mice and increased susceptibility of APAP-induced liver injuries. APAP (250 mg/kg) was intraperitoneally injected into 8-week-old C57BL/6 mice. (A) Confirmation of IDH2 knockout with an absence of mRNA expression and decreased ratio of mitochondrial NADPH to total NADPH pool in mouse liver tissue. Results are shown as the mean ± SD (n = 5 mice in each group). $^{**}p < 0.01$ between the two genotypes indicated. (B) Time-dependent analysis of ALT and AST activities. (C) C-reactive protein (CRP) expression measured by Western blot analysis. β-Actin was used as a loading control. (D) Caspase-3 activation in mouse livers by colorimetric assay. Protease activity of caspase-3 was calculated by measuring the absorbance at 405 nm. (E) In situ apoptotic cell death in liver tissue detected by TUNEL assay. Liver tissues were collected 4 h post APAP administration. (F) Western blot analysis of apoptosis-related proteins. β-Actin was used as a loading control. (G) Immunoblot analysis of activation of p38 MAPK in the liver tissues of wild-type and *idh2*$^{-/-}$ mice. β-Actin was used as a loading control. In B-D, results are shown as the mean ± SD (n = 4–5). $^{**}p < 0.01$ and $^{*}p < 0.05$ versus the WT mice exposed to APAP.

2. Materials & methods

2.1. Materials

APAP, poly(ethylene glycol) 400 (PEG), dichloro-dihydro-fluorescein diacetate (DCFH-DA), JC-1, 4-phenylbutyrate (4-PBA), Mdivi-1 and mito-TEMPO were purchased from Sigma Aldrich (St. Louis, MO). Customized PCR primers were obtained from Macrogen (Seoul, Korea). Serum alanine transaminase (ALT) and aspartate transaminase (AST) assay kits were purchased from Abnova (Taipei, Taiwan). EZ-Glutathione assay kit was purchased from DoGenBio (Seoul, Korea). In situ cell death detection kit was from Roche (Basel, Switzerland). MitoTracker, and MitoSox were purchased from Invitrogen (Eugene, OR). Mitophagy detection kit was purchased from Dojindo (Rockvile, MD). Antibodies were purchased as follows: β-Actin, C-reactive protein (CRP), JNK and C/EBP homologous protein (CHOP) (Santa Cruz Biotechnology, Santa Cruz, CA); cytochrome *c*, cleaved caspase-9, cleaved caspase-7, p38, p-p38, p-JNK, cleaved-PARP, PUMA, LC3B, Alexa488-conjugated LC3A/B, Pan-cadherin, ULK1, p-ULK1, p-mTOR (S2448), AMPK, p-AMPK, Nix, BNIP3, Parkin, PINK-1, CYP2E1, 4-hydroxynonenal (4-HNE) and HRP-conjugated secondary antibodies (Cell Signaling, Beverly, MA); ATF4 (Abcam, Cambridge, UK); Fis1 and Mfn1 (Sigma-Aldrich, St. Louis, MO); GSSG (ViroGen, Watertown, MA); OPA1 (BD Bioscience, Franklin Lakes, NJ); CYP2E1 (Millipore, Burlington, MA).

2.2. Animals

The animals used in this study were *idh2*$^{-/-}$ germ-line knockout male mice and their background strain C57BL/6 served as *idh2*$^{+/+}$ wild-type control mice. Mice were housed and bred in cages at 22 °C with 12 h light/dark cycles. Eight-week-old wild-type and *idh2*$^{-/-}$ male C57BL/6 mice, weighing 22–24 g, were used for experiments and divided into several groups of at least five mice per each group. APAP (250, 500 mg/kg), dissolved in 1:1 mixture of sterile phosphate-buffered saline (PBS) and PEG, was injected into mice intraperitoneally. Control mice received an equal quantity of sterilized PBS and PEG, only. Mito-TEMPO was dissolved in sterilized PBS and injected intraperitoneally at 2 mg/kg, 1 h before APAP injection. Mice were sacrificed at the indicated time (30 min to 24 h) after APAP treatment. Animal studies were conducted in accordance with institutional guidelines for the care and use of laboratory animals at the Animal Facility of the University Laboratory Animal Resources, Kyungpook National University.

2.3. Validation of IDH2 gene knockout

Idh2 knockout was validated by genotyping-PCR and assessment of NADPH quantities. Genomic DNA was extracted from mice liver tissues using saturated salt solution with proteinase K. Primers sequences used were as follows: *idh2* WT, forward 5′-ACTGTTCTGGAACATGCTGCC-3′, reverse 5′-TCCTCAAAGCATCAGGTACCG-3′; *idh2* KO, forward 5′-GGG TGTGACGATACATGCCTA-3′, reverse 5′-CCAGTCATAGCCGAATAG

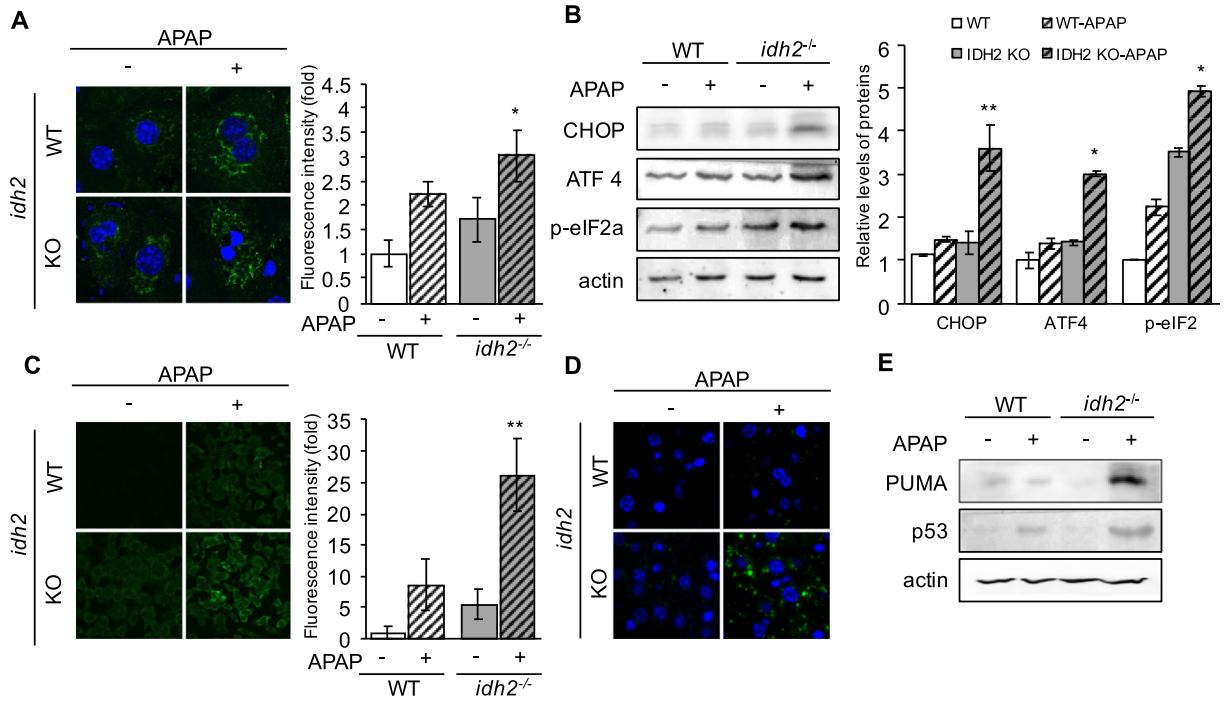

Fig. 2. APAP-treatment of *idh2*$^{-/-}$ hepatocytes exacerbates ER stress and activates related signaling pathways. (A) Immunofluorescent staining of CHOP in primary hepatocytes from wild-type and *idh2*$^{-/-}$ mice. Histograms represent quantified fluorescence intensity. (B) Expression ER stress associated protein markers measured by immunoblotting analysis. β-Actin was used as a loading control. (C) Immunofluorescent staining of PUMA in primary hepatocytes from wild-type and *idh2*$^{-/-}$ mice. Histograms represent quantified fluorescence intensity. (D) Immunofluorescent staining of p53 in primary hepatocytes. (E) Immunoblot analysis of PUMA and p53. β-Actin was used as an internal control. In A–C, results are shown as the mean ± SD (n = 3–5). $^{**}p < 0.01$ and $^{*}p < 0.05$ versus the WT mice exposed to APAP.

CCT-3′. Amplified DNA products were resolved on a 1% agarose gel with 0.01% EcoDye™ DNA staining solution (SolGent, Daejeon, South Korea). Bands were visualized using an ImageQuant LAS 500 chemiluminescence CCD camera (GE Healthcare, Buckinghamshire, UK). NADPH values were determined using the method of Zerez et al. [18] and expressed as the ratio of NADPH to the total NADP pool using the formula: [NADPH]/[NADP$^+$ + NADPH (NADPt)].

2.4. Serum analysis

Mouse blood samples were processed using serum separation tubes and centrifuged at 5000 ×*g* for 10 min. Serum alanine transaminase (ALT) and aspartate transaminase (AST) activities were determined using ALT and AST assay kits (Abnova, Taipei, Taiwan) according to the manufacturer's protocol.

2.5. Preparation of liver tissues

Mice were euthanized at the indicated time points following injection and tissues were harvested. For histochemistry and immunofluorescence, liver tissues were fixed in 4% (w/v) paraformaldehyde and embedded in paraffin. Tissues were sectioned (5 μm), deparaffinized, and rehydrated. For antigen retrieval, slides were immersed in 10 mM sodium citrate (pH 6.0) and heated to 110 °C for 10 min. For immunoblotting, liver tissues were collected and flash-frozen in liquid nitrogen.

2.6. Isolation and culture of primary hepatocytes

Primary hepatocytes were isolated as previously described [19]. Isolated primary hepatocytes were seeded on collagen coated chamber slides and incubated with William's E Medium (Thermofisher, Waltham, MA) and 5% Fetal bovine serum at 37 °C and 5% CO_2 for 24 h and treated with or without APAP, Mito-TEMPO, Z-VAD-FMK, 4-PBA and Mdivi-1.

2.7. Histochemistry and immunofluorescence

Paraffin-embedded liver sections were incubated in dry oven at 60 °C and rehydrated. Apoptosis was measured by TUNEL staining using the In situ cell death detection kit (Roche, Basel, Switzerland) according to the manufacturer's protocol. Mitochondria were observed using primary hepatocytes. Mitophagy in hepatocytes was observed using an Olympus IX83 inverted microscope. Cells were treated as according to the manufacturer's protocol and as referred to J. Konig et al. [20]. Cells were pretreated with mitophagy dye (Dojindo, Rockville, MD) for 30 min, then treated with APAP and observed after 1 h. Mitophagy dye accumulates in healthy mitochondria and exhibits a weak fluorescence. Damaged mitochondria fuse with lysosome when mitophagy is induced, and then the mitophagy dye emits a high fluorescence. For immunofluorescence, paraffin-sectioned slides or chamber slides with primary hepatocytes were incubated with specific primary antibodies at 4 °C overnight, washed with PBS 3 times, and incubated with Alexa488 or Alexa555 conjugated secondary antibody for 1 h at room temperature. Slides were then treated with anti-bleaching reagent and sealed with a cover glass. Images were analyzed using a Zeiss Axiovert 200 inverted microscope or Olympus IX83 inverted microscope.

2.8. Measurement of redox status

Total GSH was measured by the rate of formation of 5-thio-2-nitrobenzoic acid using EZ-Glutathione assay kit (DoGenBio, Seoul, Korea). Oxidized glutathione was evaluated as total GSH after treatment with 1-methyl-2-vinylpyridinium trifluoromethanesulfonate [21,22]. 4-HNE levels were measured by immunoblot analysis using anti-4-HNE antibody. The ratio of ADP to ATP was determined using a

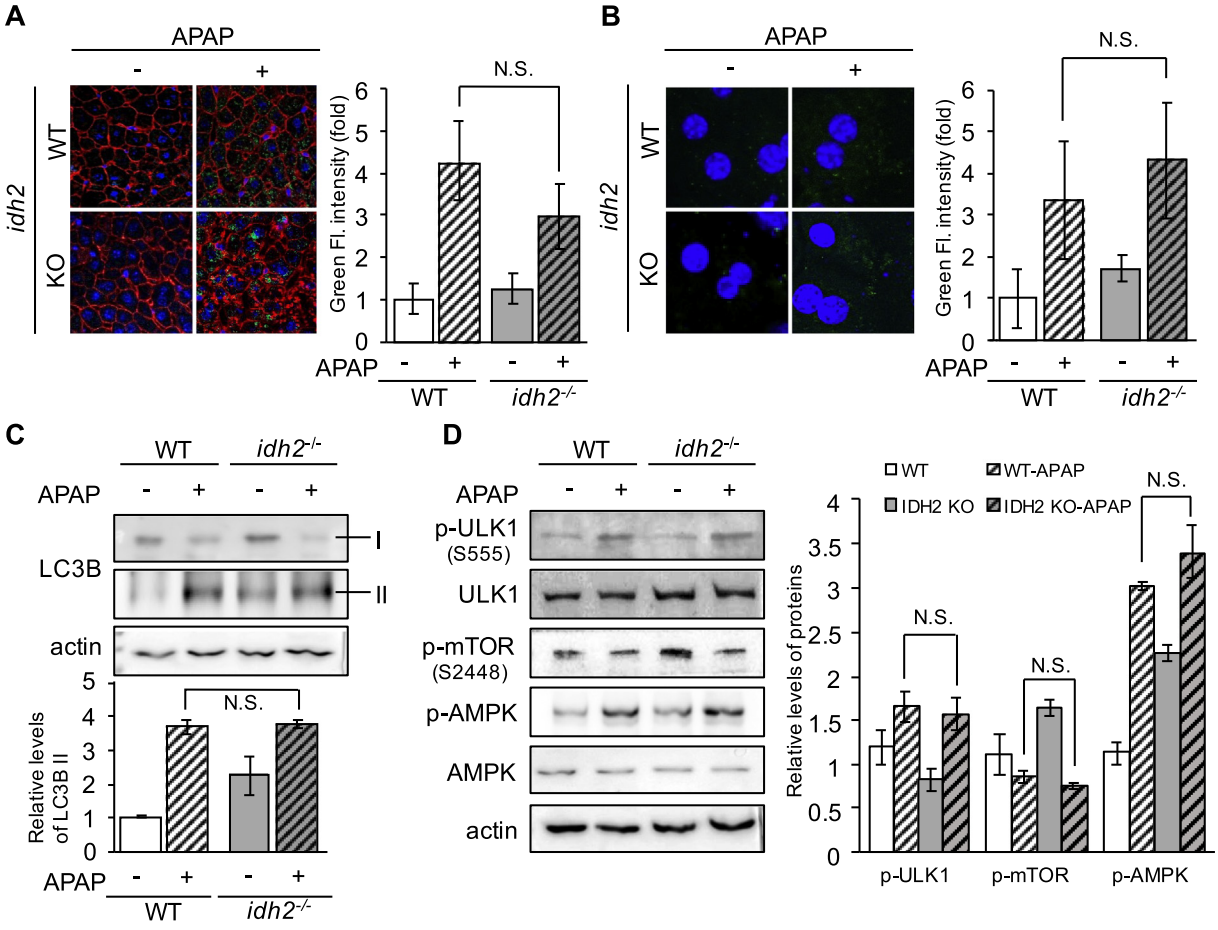

Fig. 3. Autophagy in liver tissues from mice treated with 1 mM APAP. (A) Immunofluorescence staining of LC3A/B (green) and Pan-cadherin (red) in liver tissues and (B) primary hepatocytes. Nuclei were stained with DAPI (blue). (C) Western blot analysis for LC3B protein. β-Actin was used as an internal control. (D) Western blot analysis of autophagy-related proteins in liver tissues harvested 2 h post APAP treatment. β-Actin was used as a loading control. In A-D, results are shown as the mean ± SD (n = 3–5). N.S., not statistically significant.

commercial ADP/ATP assay kit (Abcam, Cambridge, UK) according to the manufacturer's protocol. Mitochondrial membrane potential was assessed using the fluorescent probe, JC-1, and a Zeiss Axiovert 200 inverted microscope and quantified using Image J software. Mitochondrial ROS was detected using mitoSOX with an inverted microscope.

2.9. Measurement of mitochondrial DNA damage

Mitochondrial DNA (mtDNA) damage was measured by quantitative PCR as described by Furda et al. [23]. MtDNA were extracted from mice livers using a Genomic DNA buffer set kit and a Genomic tip (Qiagen,Venlo, Netherlands). Sequences of the primers used were as follows: 10-kb mitochondria fragment, forward 5′-GCC AGC CTG ACC CAT AGC CAT ATT AT-3′, reverse 5′-GAG AGA TTT TAT GGG TGT ATT GCG G-3′; 117-bp mitochondria fragment, forward 5′-CCC AGC TAC TAC CAT CAT TCA AGT-3′, reverse 5′-GA T GGT TTG GGA GA T TGG TTG A TG-3′. Amplified mtDNA were incubated with Picogreen and fluorescence detected using a SPARK 10M Multi plate reader (TECAN, Männedorf, Switzerland). Lesion frequencies were represented as raw fluorescence values of amplified large mitochondrial fragments normalized small mitochondrial fragments.

2.10. Immunoblot analysis

Liver tissue extracts were separated on 8–12% SDS-polyacrylamide gels and transferred to nitrocellulose membranes. The membranes were probed with specific primary antibodies overnight at 4 °C, washed, and then labeled with horseradish peroxidase-labeled secondary antibodies and an enhanced chemiluminescence detection kit (GE Healthcare, Buckinghamshire, UK). Luminescence was visualized using ImageQuant LAS 500 chemiluminescence CCD camera.

2.11. Statistical analysis

All experiments were performed at least three times. Results are presented as the mean ± standard deviation (SD). Two-tailed *t*-test was used to determine statistical significance between two mean values. $P < 0.05$ was considered statistically significant.

3. Results

3.1. Knockout of IDH2 increases susceptibility to APAP-induced liver injury in C57BL/6 mice

Depletion of IDH2 in mice was confirmed by PCR genotyping, which revealed shortening of IDH2 mRNA in *idh2*$^{-/-}$ mice, and enzymatic analysis for measurement of NADPH. The ratio of NADPH versus the total pool of NADP + NADPH was significantly decreased in the livers of *idh2*$^{-/-}$ mice (Fig. 1A). To test whether IDH2 plays a role in APAP-induced liver injury, APAP was administered to *idh2*$^{+/+}$ and *idh2*$^{-/-}$ mice intraperitoneally at a dose of 250 mg/kg and the mice were serially sacrificed between 0 (pre-challenge) and 24 h post-injection. ALT and AST activities were significantly increased in serum of *idh2*$^{-/-}$

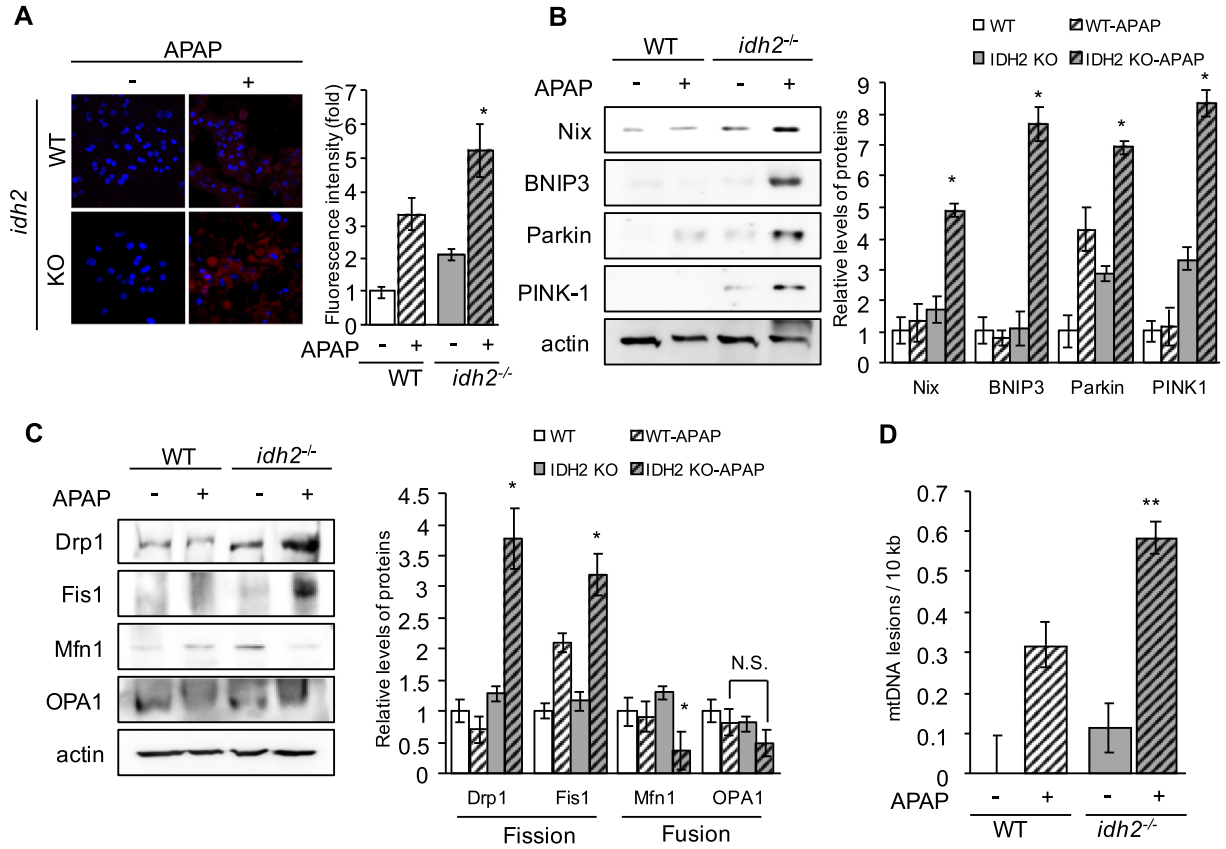

Fig. 4. Mitophagy caused by mitochondrial dysfunction in liver tissues of *idh2*$^{-/-}$ mice treated with 1 mM APAP. (A) Mitophagy in primary hepatocytes using a mitophagy detection kit and observed by microscopy. (B) Western blot analysis of mitophagy related proteins in liver tissues. β-Actin was used as a loading control. (C) Immunoblot analysis of mitochondrial fusion and fission markers. β-Actin was used as an internal control. (D) Quantitative PCR analysis of mitochondrial DNA damage in liver tissue. Results are shown as the mean ± SD (n = 4–5). $^{**}p < 0.01$ and $^{*}p < 0.05$ versus the WT mice exposed to APAP. N.S., not statistically significant.

mice compared to that from of *idh2*$^{+/+}$ mice (Fig. 1B). The hepatic level of CRP has been reported as an inflammatory biomarker for acute toxicity [24]. Western blot analysis showed increased levels of CRP in *idh2*$^{-/-}$ mice following APAP treatment (Fig. 1C).

A higher dose of APAP (500 mg/kg) on mice also induced elevations of ALT, AST and CRP but there were no significant differences between *idh2*$^{+/+}$ and *idh2*$^{-/-}$ mice (Supplementary Fig. 1). Colorimetric detection of caspase activities in liver tissues indicated that *idh2*$^{-/-}$ mice were more sensitive to APAP-induced caspase-3 activation than wild-type mice (Fig. 1D). A significantly higher number of TUNEL-positive hepatocytes was observed in *idh2*$^{-/-}$ mice compared to *idh2*$^{+/+}$ mice treated with APAP (Fig. 1E). Furthermore, proteolytic cleavage of proapoptotic markers PARP, caspase-9 and caspase-7, and release of cytochrome *c* from mitochondria were remarkably increased in APAP-treated *idh2*$^{-/-}$ mice compared to wild-type mice (Fig. 1F). The level of stress-induced JNK/p38 activation was also higher in *idh2*$^{-/-}$ mice treated with APAP compared control mice (Fig. 1G). To confirm APAP-induced apoptotic cell death in *idh2*$^{-/-}$ mice, the pancaspase inhibitor Z-VAD-FMK (Z-VAD) was added to *idh2*$^{-/-}$ primary hepatocytes. Activated caspase-3 was not detected and cell viability after APAP treatment was significantly improved in the presence of Z-VAD (Supplementary Fig. 2B and Fig. 2C). Collectively, these results show that IDH2 deficiency increases susceptibility to APAP-induced liver injury in mice via stress-induced activation of the JNK/p38 signaling, thereby inducing hepatic apoptosis. However, the mechanisms of enhanced APAP-induced liver injury in the absence of IDH2 remained unclear, thus we further explored APAP-induced hepatotoxicity in *idh2*$^{-/-}$ mice.

3.2. Knockout of IDH2 exacerbates ER stress under exposure to APAP

ER stress activates the JNK/p38 pathway resulting in apoptotic cell death [25]. Therefore, we examined ER stress-induced signaling activation in *idh2*$^{-/-}$ mice treated with APAP. ER stress induces transcription factor CHOP that is probably not only the most sensitive marker of ER stress, but also contributes to ER stress-induced apoptosis [26,27]. Peak CHOP expression was observed in *idh2*$^{-/-}$ primary hepatocytes treated with 1 mM APAP for 2 h as measured by immunofluorescence staining with anti-CHOP antibodies (Fig. 2A). Induction of CHOP is strongly dependent on ATF4 and phosphorylation of eIF2a as a branch of the unfolded protein response (UPR) to ER stress [28]. As shown in Fig. 2B, protein expression in liver tissues revealed IDH2 deficiency increases sensitivity to APAP-induced ER stress. ER stress also induces PUMA at the transcription level in a manner dependent on p53. PUMA is a member of the BH3-protein family, which induces cytochrome *c* release from mitochondria [29]. Fluorescence microscopy revealed increased expression of PUMA and p53 following APAP treatment, especially in *idh2*$^{-/-}$ hepatocytes (Fig. 2C and D). Immunoblot analysis of liver lysates confirmed the results from primary hepatocytes (Fig. 2E). However, ER stress as a reason of cell death is still unclear. Primary hepatocytes from *idh2*$^{-/-}$ mice were treated with ER stress inhibitor 4-PBA and expression of cleaved-capsase-3 was significantly decreased when 4-PBA was administered (Supplementary Fig. 2D). These results suggest that elevated apoptosis in IDH2 deficient mice (Fig. 1D–G) was induced by increased ER stress and subsequent activation of signaling pathways involving CHOP and PUMA. How IDH2 deletion increases ER stress in response to APAP treatment is not clear. Autophagy has emerged as an essential protective mechanism

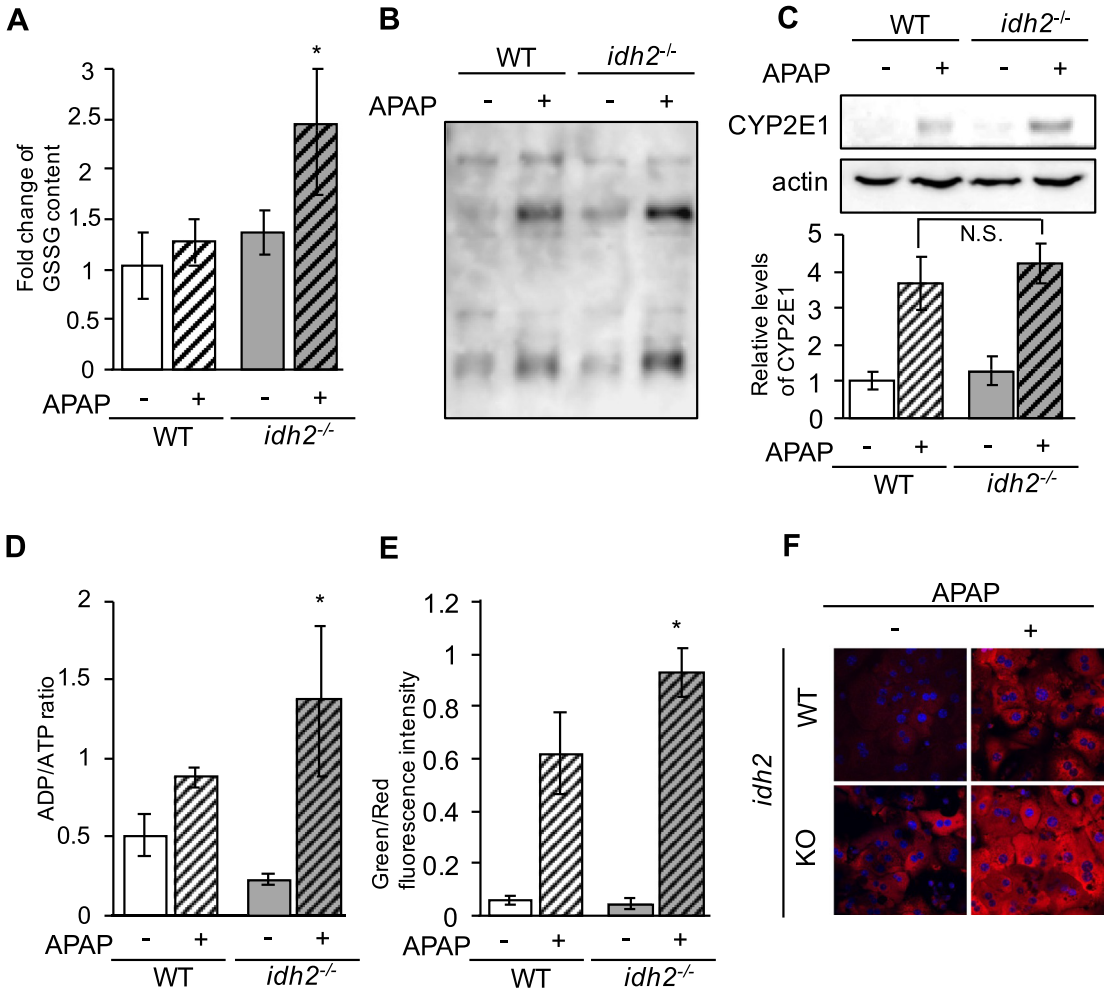

Fig. 5. Modulation of redox status in liver tissues from of *idh2*$^{-/-}$ mice. (A) Redox status in liver tissues measured by enzymatic assay. The fold change of oxidized glutathione (GSSG) is presented. (B) Immunoblot analysis of 4-HNE, a major lipid peroxidation product in liver tissues. (C) CYP2E1 expression in livers of *idh2*$^{-/-}$ mice treated with APAP by western blot. β-Actin was used as an internal control. (D) ADP to ATP ratio as a measure of mitochondrial function in liver tissues from *idh2*$^{-/-}$ mice assessed using an ADP/ATP assay kit. (E) Mitochondrial membrane potential APAP-treated *idh2*$^{-/-}$ primary hepatocytes stained with JC-1. Fluorescence intensity was plotted using Image J software. (F) Mitochondrial ROS in *idh2*$^{-/-}$ primary hepatocytes imaged using MitoSox staining light microscopy. In A and C-E, results are shown as the mean ± SD (n = 3–5). *$p < 0.05$ versus the WT mice exposed to APAP. N.S., not statistically significant.

during ER stress and recent studies have shown that ER stress can either stimulate or inhibit autophagy [30]. Therefore, we next examined autophagy in *idh2*$^{-/-}$ mice.

3.3. APAP induces autophagy in mouse liver

Recent investigations reported that APAP treatment leads to autophagy induction, both in vivo and in vitro [31,32]. Activation of autophagy also has protective effects on APAP-induced hepatotoxicity [33]. To demonstrate autophagy induction upon APAP treatment, LC3 puncta in liver tissues were examined by confocal microscope. Formation of autophagosomes in liver tissues was increased after APAP treatment in both *idh2*$^{-/-}$ and wild-type mice (Fig. 3A). However, there was no significant difference between IDH2 deficient mice and wild-type mice. Morphological disruption, determined by pan-cadherin antibody detection of membrane integrity in liver tissues, has previously been observed in *idh2*$^{-/-}$ mice treated with APAP [34]. Cadherin degradation occurs during apoptosis [35], thus our findings of hepatic apoptosis in APAP-treated *idh2*$^{-/-}$ mice (Fig. 1D–G) is well supported. Formation of LC3 puncta in primary hepatocytes (Fig. 3B) and western blot analysis of LC3B in liver tissues (Fig. 3C) further confirmed the data presented in Fig. 3A. Recent studies have demonstrated that autophagy induction was promoted through activation of AMPK and ULK1 phosphorylation due to an energy deficit when treated with APAP [36]. Strengthened autophagy signaling activation following APAP administration was observed by immunoblot in mouse liver (Fig. 3D). However, no significant differences between *idh2*$^{-/-}$ and wild-type mice were observed. As described above, recent studies have shown that autophagy has protective effects against APAP-induced hepatotoxicity [31,37] which could explain why wild-type hepatocytes are less sensitive to APAP-induced hepatotoxicity. However, this does not fully describe the pathways involved in *idh2*$^{-/-}$ hepatocyte cell death. Because IDH2 is mitochondrial enzyme, it is possible that deletion of IDH2 might impact on mitochondria. Therefore, we investigated mitochondria-specific autophagy, or mitophagy.

3.4. Mitochondrial dysfunction is increased in idh2$^{-/-}$ mice following APAP treatment

Mitophagy performs an elimination role for mitochondria that have become dysfunctional due to oxidative stress and DNA damage. Mitophagy involves fusion of autophagosome, including engulfed mitochondria, with the lysosome, leading to degradation of the encapsulated mitochondria. Fusion of mitochondria and lysosome, indicated by red fluorescence, was markedly intensified in APAP-treated *idh2*$^{-/-}$ primary hepatocytes compared to non-treated *idh2*$^{-/-}$

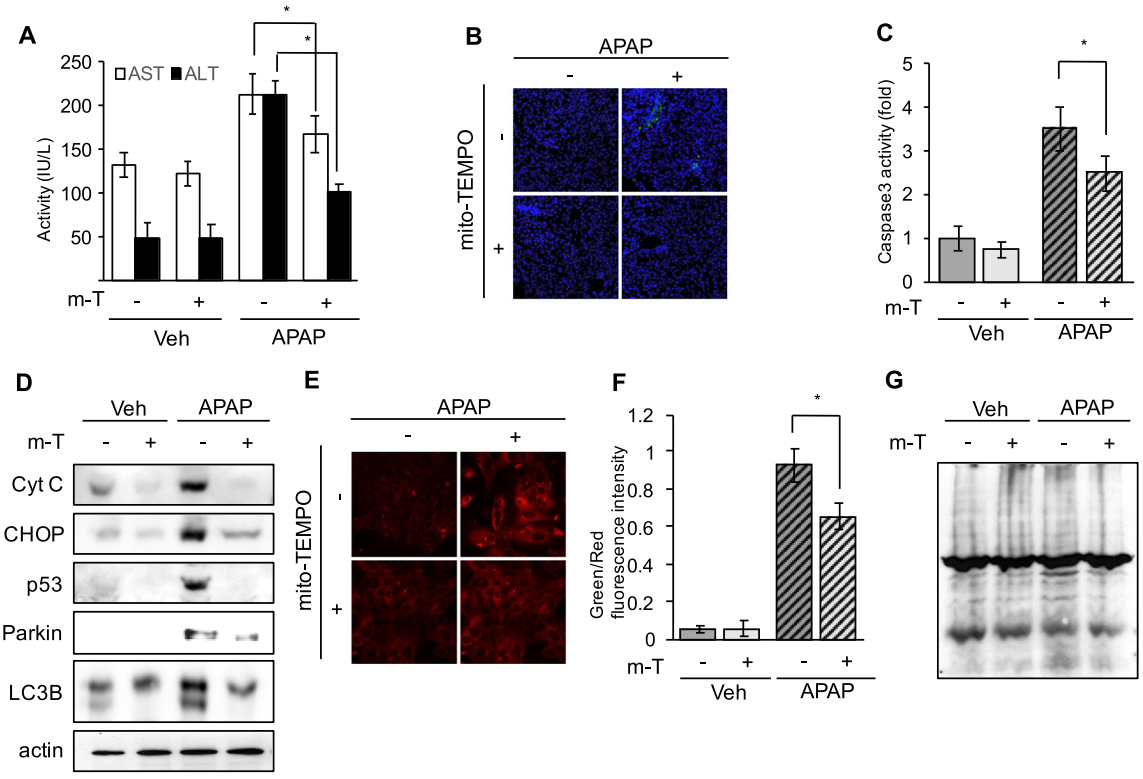

Fig. 6. Protective effects of mito-TEMPO against APAP-induced liver injury in *idh2*$^{-/-}$ mice. Mice were treated with mito-TEMPO (2 mg/kg, i.p.) 2 h prior to treatment with APAP (250 mg/kg, i.p.) (A) Serum ALT and AST activity measured using Abnova serum assay kit. (B) Apoptotic cell death in liver tissues detected using an In situ cell detection kit. (C) Activation of caspase-3 in mouse livers measured by colorimetry. Samples were read at 405 nm (D) Western blot analysis of mitophagy-associated signaling molecules, cytochrome *c*, CHOP, p53, LC3B and Parkin in mito-TEMPO-treated *idh2*$^{-/-}$ mouse liver. (E) Mitophagy in *idh2*$^{-/-}$ primary hepatocytes imaged by light microscopy with mitophagy detection kit. (F) MMP of *idh2*$^{-/-}$ primary hepatocytes using JC-1 staining and light microscopy. Fluorescence was quantified using Image J software. (G) APAP-induced nitrotyrosine formation in the *idh2*$^{-/-}$ hepatocytes was measured by immunoblot analysis. In A, C and F, results are shown as the mean ± SD (n = 3–5). *$p < 0.05$. m-T, mito-TEMPO.

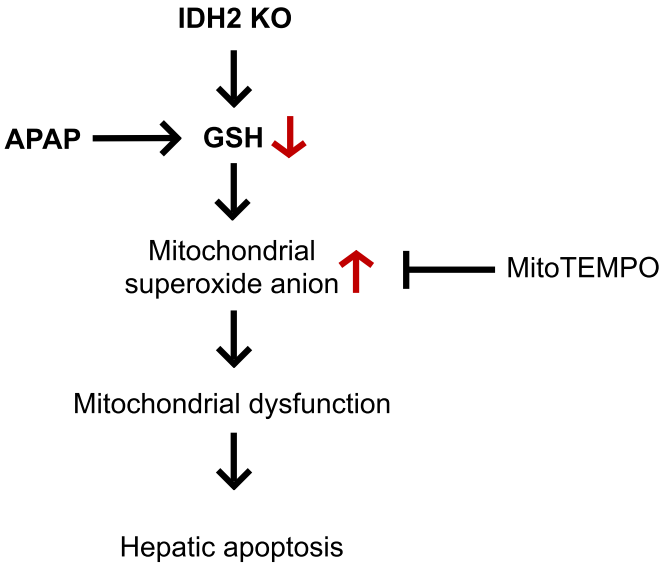

Fig. 7. Schematic diagram showing how IDH2 deficiency promotes APAP-induced hepatic apoptosis and the protective effects of mito-TEMPO against APAP-induced hepatic apoptosis.

hepatocytes (Fig. 4A), while fluorescence intensity in wild-type hepatocytes was not significantly increased following APAP treatment. Protein expression of markers related to mitophagy pathways, including PINK1/Parkin associated pathways and BNIP3/Nix pathways, were also markedly increased in *idh2*$^{-/-}$ livers from mice treated with APAP (Fig. 4B). Reduced membrane potential in fragmented mitochondria is a precondition of mitophagy induction [38]. Mitochondrial morphology is closely related to mitochondrial dynamics. Mitochondrial dynamics are a quality control system for maintaining healthy mitochondria by facilitating the removal of damaged mitochondria from the cell [39]. As components of this mitochondrial-maintenance system, we examined the expression of fission marker, Drp1/Fis1, and fusion marker, Opa1/Mfn1 by immunoblotting. Consistent with the data in Fig. 4C, expression of fission markers was increased in livers from *idh2*$^{-/-}$ mice compared to livers from wild-type mice treated with APAP. This mitochondrial dynamics, which is biased toward fission, represents *idh2*$^{-/-}$ primary hepatocytes treated with APAP have more fragmented mitochondria than in wild-type primary cells treated with APAP. Mdivi-1, which reduces Drp1 levels and consequently inhibits mitochondrial dysfunction, was treated to *idh2*$^{-/-}$ primary hepatocytes to claim responsibility for the mitochondrial dysfunction-induced apoptosis. Decreased level of activated caspase3 after Mdivi-1 treatment in Supplementary Fig. 2E demonstrated the causality between mitochondrial dysfunction and cell death. This indicates that the absence of IDH2 makes mitochondria vulnerable during APAP administration. It has been reported that the mitochondrial dysfunction and selective deletion of the defective mitochondria is induced when deleterious mtDNA damage accumulates [40]. Therefore, we quantitated the generation of mtDNA damage. Lesion frequencies on mtDNA, obtained by quantitative PCR, were significantly higher in livers taken from *idh2*$^{-/-}$ compared to the livers of wild-type mice. IDH2 serves as a donor of NADPH to mitochondria to maintain the antioxidant system, as previously described. In the absence of IDH2, the antioxidant system is ablated causing further oxidative stress and excessive mtDNA damage, and this could explain the increased mitochondrial dysfunction

in *idh2*$^{-/-}$ mice.

3.5. Redox status is altered in hepatocytes of *idh2*$^{-/-}$ mice

Cells are equipped with complicated networks of antioxidant defense systems and IDH2 functions as a provider of NADPH for NADPH-dependent antioxidant enzymes. Thus, IDH2 plays a crucial role in regulating mitochondrial redox balance and reducing oxidative stress in cells. In Fig. 1A, we have shown diminished NADPH levels in livers from *idh2*$^{-/-}$ liver. Because NADPH is essential for the regeneration of GSH and reduction of the thioredoxin system, and GSH depletion is major factor in APAP-induced cytotoxicity, we measured the content of GSSG, an important parameter of GSH turnover, in mouse liver. Oxidized GSH was increased and turnover to its reduced form was notably reduced in the livers of *idh2*$^{-/-}$ mice treated with APAP (Fig. 5A). To evaluate cellular oxidative damage, we measured the protein expression of 4-HNE, a major lipid peroxidation product. 4-HNE was significantly higher in *idh2*$^{-/-}$ mice compared to wild-type mice (Fig. 5B). Taken together, these results suggest that IDH2 deletion amplified oxidative stress in the livers of APAP-treated mice.

We next observed the effect of mitochondria in oxidative stress and mitochondrial ROS generation. It has been broadly reported that the activation of CYP2E1 is one of the major contributors to APAP-induced hepatotoxicity [41]. CYP2E1 is the primary enzyme for ROS generation and bio-activation of APAP, and its activity is increased following APAP treatment [42]. We confirmed the increased expression of CYP2E1 in the livers of mice treated with APAP and there was no significant difference between *idh2*$^{-/-}$ and wild-type mice (Fig. 5C). We have shown APAP-induced mtDNA damage was significant in *idh2*$^{-/-}$ mice. Thus, to test whether mitochondria were functional or not, we examined the ratio of ADP to ATP, and mitochondrial membrane potential (MMP). The ratio of ADP to ATP was higher in IDH2 deficient primary hepatocytes treated with APAP (Fig. 5D). The MMP of *idh2*$^{-/-}$ primary hepatocytes treated with APAP was lower than that of non-treated cell, as indicated by a more intense green fluorescent signal (Fig. 5E). Higher cytosolic ADP/ATP ratio and lower MMP represent suppressed mitochondrial function [43,44]. Thus APAP-treated *idh2*$^{-/-}$ hepatocytes were shown to have mitochondrial dysfunction. Fig. 5F shows a marked increase in mitoSox fluorescence intensity after treatment of *idh2*$^{-/-}$ primary hepatocytes with APAP and this fluorescence increase was less pronounced in wild-type cells. This suggests that IDH2 deficiency promotes the production of mitochondrial ROS in APAP-treated hepatocytes. Collectively, although ROS are produced in both models, an absence of IDH2 accelerates GSH depletion and weakens regulation of the antioxidant system, leading to oxidative damage.

3.6. Mito-TEMPO protects against APAP-induced liver injury in IDH2 deficient mice

Our previous study suggested that mito-TEMPO reduced oxidative stress by scavenging mitochondrial superoxide, specifically [15]. Therefore, we evaluated the protective effects of this mitochondrial ROS scavenger during APAP-induced hepatotoxicity. *Idh2*$^{-/-}$ mice treated with APAP only, had higher serum ALT and AST activity than *idh2*$^{-/-}$ mice treated with APAP plus mito-TEMPO (Fig. 6A). TUNEL staining of liver tissue from *idh2*$^{-/-}$ mice treated with or without APAP and mito-TEMPO showed that mito-TEMPO reduced APAP-induced hepatotoxicity in *idh2*$^{-/-}$ mice, with no detectable toxicity to hepatocytes from mito-TEMPO administration (Fig. 6B). The protective effect of mito-TEMPO against APAP-induced apoptosis is also demonstrated by colorimetric assay showing reduced caspase-3 activity (Fig. 6C). The release of cytochrome *c* from mitochondria, and protein expression of CHOP and p53, activation of LC3B and Parkin expression in the tissues of APAP/mito-TEMPO-treated mice were attenuated compared to that seen in mice treated with APAP only (Fig. 6D). Fluorescent images also showed amelioration of excessive mitophagy caused by mitochondrial dysfunction in hepatocytes by mito-TEMPO treatment (Fig. 6E). MMP measurement showed that mito-TEMPO administration mitigated APAP-induced mitochondrial dysfunction in hepatocytes from *idh2*$^{-/-}$ mice (Fig. 6F). Furthermore, Mito-TEMPO treatment protected against mitochondrial superoxide anion formation as indicated by elimination of APAP-induced nitrotyrosine staining in the *idh2*$^{-/-}$ hepatocytes (Fig. 6G), consistent with the previous report that the effective dismutation of superoxide by Mito-TEMPO can prevent peroxynitrite formation [9].

4. Discussion

This study presents experimental evidence that IDH2 deficiency accelerates APAP-induced hepatotoxicity. An absence of IDH2 resulted in diminished NADPH, which is essential for GSH turnover and reduction of the thioredoxin system. Many studies have already demonstrated that APAP administration induces a shortage of GSH. IDH2 deficient cells are not able to replenish GSH, leaving the cells more susceptible to further APAP-induced GSH impoverishment. When APAP was administered, CYP2E1, the primary enzyme of APAP bioactivation and associated ROS generation, was activated at the same level in both models. However, the level of oxidative stress was higher in IDH2 deficient hepatocytes than in wild-type cells. This appears to be the consequence of reduced oxidative capacity following GSH depletion. Thus, a fundamental shortage of GSH in IDH2 deficient cells renders them fragile and more sensitive to ROS generation and oxidative stress.

Previous studies have demonstrated that production of ROS by mitochondria and oxidative stress induces mtDNA damage, which in turn causes respiratory chain dysfunction and further increases in ROS generation. This catastrophic cycle leads to mitochondrial dysfunction [45–47]. Our results using an APAP-treated IDH2 deficient mouse model mirror this deleterious process. To maintain mitochondrial homeostasis in this model, mitochondrial dynamics were seen to shift toward fission rather than fusion to delete damaged mitochondria. Mitophagy was also activated. Mitophagy is defined to be the selective degradation of defective mitochondria by autophagy, and the increase in the degraded mitochondria is proportional to the activation of apoptosis. However, no significant difference in autophagy induction after APAP treatment was observed between IDH2 deficient and wild-type cells in this study, which represents the activation of the core autophagy machinery remains largely the same between the two genotypes in the response to APAP treatment (Fig. 3). Autophagy and mitophagy themselves are protective mechanisms to remove APAP adducts, damaged protein and mitochondria. When these mechanisms are activated, they protect against APAP-induced liver failure. However, the increase in the lysosomal degradation of the defective mitochondria from the APAP-treated *idh2*$^{-/-}$ hepatocytes leads to the increased susceptibility to the apoptotic cell death in the liver tissues. Furthermore, excessive activation of autophagy or mitophagy has been shown to be a cause of cell death. Mitophagy associated proteins, BNIP3 and NIX are also known cause mitochondrial depolarization and cell death [48]. Lim et al. demonstrated that mitochondrial dysfunction can induce ER stress [49]. ER stress also interferes with mitochondria, leading to mitochondrial dysfunction and apoptosis [50].

In conclusion, APAP administration in IDH2 deficient mouse model resulted in mitochondrial damage and mitophagy beyond protection, resulting in induction of ER stress. ER stress interfered with the mitochondria to further induce mitochondrial depolarization. This status ultimately leads to apoptotic cell death, and ultimately, liver failure (Fig. 7). In this study, we confirmed that IDH2 plays a role in protecting hepatocytes against APAP-induced liver damage by balancing the oxidative status in cells. These findings demonstrate that the complex linkages and functions of the antioxidant system are crucial to liver health.

Transparency document

The Transparency document associated with this article can be found, in online version.

Acknowledgment

This work was supported by the National Research Foundation of Korea (NRF) grants funded by the Korea Government (MSIP) (NRF-2015R1A4A1042271). No potential conflicts of interest relevant to this article are reported.

Appendix A. Supplementary data

Supplementary data to this article can be found online at https://doi.org/10.1016/j.bbadis.2019.05.012.

References

[1] W. Bernal, W.M. Lee, J. Wendon, F.S. Larsen, R. Williams, Acute liver failure: a curable disease by 2024? J. Hepatol. 62 (2015) S112–S120.
[2] A.M. Larson, J. Polson, R.J. Fontana, T.J. Davern, E. Lalani, L.S. Hynan, J.S. Reisch, F.V. Schiodt, G. Ostapowicz, A.O. Shakil, W.M. Lee, Acute Liver Failure Study, Acetaminophen-induced acute liver failure: results of a United States multicenter, prospective study, Hepatolology 42 (2005) 1364–1372.
[3] K. Du, A. Ramachandran, H. Jaeschke, Oxidative stress during acetaminophen hepatotoxicity: sources, pathophysiological role and therapeutic potential, Redox Biol. 10 (2016) 148–156.
[4] A.J. Shuhendler, K. Pu, L. Cui, J.P. Uetrecht, J. Rao, Real-time imaging of oxidative and nitrosative stress in the liver of live animals for drug-toxicity testing, Nat. Biotechnol. 32 (2014) 373–380.
[5] M.L. Bajt, T.R. Knight, J.J. Lemasters, H. Jaeschke, Acetaminophen-induced oxidant stress and cell injury in cultured mouse hepatocytes: protection by N-acetyl cysteine, Toxicol. Sci. 80 (2004) 343–349.
[6] L.P. James, P.R. Mayeux, J.A. Hinson, Acetaminophen-induced hepatotoxicity, Drug Metab. Dispos. 31 (2003) 1499–1506.
[7] P.D. Ray, B.W. Huang, Y. Tsuji, Reactive oxygen species (ROS) homeostasis and redox regulation in cellular signaling, Cell. Signal. 24 (2012) 981–990.
[8] Y. Kushnareva, A.N. Murphy, A. Andreyev, Complex I-mediated reactive oxygen species generation: modulation by cytochrome c and NAD(P)$^+$ oxidation-reduction state, Biochem. J. 368 (2002) 545–553.
[9] K. Du, A. Ramachandran, J.L. Weemhoff, H. Chavan, Y. Xie, P. Krishnamurthy, H. Jaeschke, Metformin protects against acetaminophen hepatotoxicity by attenuation of mitochondrial oxidant stress and dysfunction, Toxicol. Sci. 154 (2016) 214–226.
[10] B. Halliwell, J.M. Gutteridge, Oxygen toxicity, oxygen radicals, transition metals and disease, Biochem. J. 219 (1984) 1–14.
[11] C. Saito, C. Zwingmann, H. Jaeschke, Novel mechanisms of protection against acetaminophen hepatotoxicity in mice by glutathione and N-acetylcysteine, Hepatology 51 (2010) 246–254.
[12] D. Mustacich, G. Powis, Thioredoxin reductase, Biochem. J. 346 (2000) 1–8.
[13] S.Y. Park, S.M. Lee, S.W. Shin, J.-W. Park, Inactivation of mitochondrial NADP$^+$-dependent isocitrate dehydrogenase by hypochlorous acid, Free Rad. Res. 42 (2008) 467–473.
[14] S. Kim, S.Y. Kim, H.J. Ku, Y.H. Jeon, H.W. Lee, J. Lee, T.K. Kwon, K.M. Park, J.-W. Park, Suppression of tumorigenesis in mitochondrial NADP(+)-dependent isocitrate dehydrogenase knock-out mice, Biochim. Biophys. Acta 1842 (2014) 135–143.
[15] H. Kim, S.H. Kim, H. Cha, S.R. Kim, J.H. Lee, J.-W. Park, IDH2 deficiency promotes mitochondrial dysfunction and dopaminergic neurotoxicity: implications for Parkinson's disease, Free Rad. Res. 50 (2016) 853–860.
[16] H. Cha, S. Lee, S. Hwan Kim, H. Kim, D.S. Lee, H.S. Lee, J.H. Lee, J.-W. Park, Increased susceptibility of IDH2-deficient mice to dextran sodium sulfate-induced colitis, Redox Biol. 13 (2017) 32–38.
[17] J.H. Park, H.J. Ku, J.H. Lee, J.-W. Park, Disruption of IDH2 attenuates lipopolysaccharide-induced inflammation and lung injury in an alpha-ketoglutarate-dependent manner, Biochem. Biophys. Res. Commun. 503 (2018) 798–802.
[18] C.R. Zerez, D.E. Moul, E.G. Gomez, V.M. Lopez, A.J. Andreoli, Negative modulation of Escherichia coli NAD kinase by NADPH and NADH, J. Bacteriol. 169 (1987) 184–188.
[19] H. Kim, J.H. Pan, S.H. Kim, J.H. Lee, J.-W. Park, Chlorogenic acid ameliorates alcohol-induced liver injuries through scavenging reactive oxygen species, Biochimie 150 (2018) 131–138.
[20] J. Konig, C. Ott, M. Hugo, T. Jung, A.L. Bulteau, T. Grune, A. Hohn, Mitochondrial contribution to lipofuscin formation, Redox Biol. 11 (2017) 673–681.
[21] C.R. Zerez, S.J. Lee, K.R. Tanaka, Spectrophotometric determination of oxidized and reduced pyridine nucleotides in erythrocytes using a single extraction procedure, Anal. Biochem. 164 (1987) 367–373.
[22] T.P. Akerboom, H. Sies, Assay of glutathione, glutathione disulfide, and glutathione mixed disulfides in biological samples, Methods Enzymol. 77 (1981) 373–382.
[23] A. Furda, J.H. Santos, J.N. Meyer, B. van Houten, Quantitative PCR-based measurement of nuclear and mitochondrial DNA damage and repair in mammalian cells, Methods Mol. Biol. 1105 (2014) 419–437.
[24] A. Zambon, P. Gervois, P. Pauletto, J.C. Fruchart, B. Staels, Modulation of hepatic inflammatory risk markers of cardiovascular diseases by PPAR-alpha activators: clinical and experimental evidence, Arterioscler. Thromb. Vasc. Biol. 26 (2006) 977–986.
[25] N.J. Darling, S.J. Cook, The role of MAPK signalling pathways in the response to endoplasmic reticulum stress, Biochim. Biophys. Acta 1843 (2014) 2150–2163.
[26] H. Zinszner, M. Kuroda, X. Wang, N. Batchvarova, R.T. Lightfoot, H. Remotti, J.L. Stevens, D. Ron, CHOP is implicated in programmed cell death in response to impaired function of the endoplasmic reticulum, Genes Dev. 12 (1998) 982–995.
[27] D. Uzi, L. Barda, V. Scaiewicz, M. Mills, T. Mueller, A. Gonzalez-Rodriguez, A.M. Valverde, T. Iwawaki, Y. Nahmias, R. Xavier, R.T. Chung, B. Tirosh, O. Shibolet, CHOP is a critical regulator of acetaminophen-induced hepatotoxicity, J. Hepatol. 59 (2013) 495–503.
[28] E. Szegezdi, S.E. Logue, A.M. Gorman, A. Samali, Mediators of endoplasmic reticulum stress-induced apoptosis, EMBO Rep. 7 (2006) 880–885.
[29] J. Li, B. Lee, A.S. Lee, Endoplasmic reticulum stress-induced apoptosis: multiple pathways and activation of p53-up-regulated modulator of apoptosis (PUMA) and NOXA by p53, J. Biol. Chem. 281 (2006) 7260–7270.
[30] H.O. Rashid, R.K. Yadav, H.R. Kim, H.J. Chae, ER stress: autophagy induction, inhibition and selection, Autophagy 11 (2015) 1956–1977.
[31] Y. Igusa, S. Yamashina, K. Izumi, Y. Inami, H. Fukada, M. Komatsu, K. Tanaka, K. Ikejima, S. Watanabe, Loss of autophagy promotes murine acetaminophen hepatotoxicity, J. Gastroenterol. 47 (2012) 433–443.
[32] H.M. Ni, N. Boggess, M.R. McGill, M. Lebofsky, P. Borude, U. Apte, H. Jaeschke, W.X. Ding, Liver-specific loss of Atg5 causes persistent activation of Nrf2 and protects against acetaminophen-induced liver injury, Toxicol. Sci. 127 (2012) 438–450.
[33] H.M. Ni, A. Bockus, N. Boggess, H. Jaeschke, W.X. Ding, Activation of autophagy protects against acetaminophen-induced hepatotoxicity, Hepatology 55 (2012) 222–232.
[34] K. Vleminckx, R. Kemler, Cadherins and tissue formation: integrating adhesion and signaling, Bioessays 21 (1999) 211–220.
[35] S.N. Hartland, F. Murphy, R.L. Aucott, A. Abergel, X. Zhou, J. Waung, N. Patel, C. Bradshaw, J. Collins, D. Mann, R.C. Benyon, J.P. Iredale, Active matrix metalloproteinase-2 promotes apoptosis of hepatic stellate cells via the cleavage of cellular N-cadherin, Liver Int. 29 (2009) 966–978.
[36] X. Chao, H. Wang, H. Jaeschke, W.X. Ding, Role and mechanisms of autophagy in acetaminophen-induced liver injury, Liver Int. 38 (2018) 1363–1374.
[37] H.M. Ni, M.R. McGill, X. Chao, K. Du, J.A. Williams, Y. Xie, H. Jaeschke, W.X. Ding, Removal of acetaminophen protein adducts by autophagy protects against acetaminophen-induced liver injury in mice, J. Hepatol. 65 (2016) 354–362.
[38] G. Twig, A. Elorza, A.J. Molina, H. Mohamed, J.D. Wikstrom, G. Walzer, L. Stiles, S.E. Haigh, S. Katz, G. Las, J. Alroy, M. Wu, B.F. Py, J. Yuan, J.T. Deeney, B.E. Corkey, O.S. Shirihai, Fission and selective fusion govern mitochondrial segregation and elimination by autophagy, EMBO J. 27 (2008) 433–446.
[39] A.Y. Seo, A.M. Joseph, D. Dutta, J.C. Hwang, J.P. Aris, C. Leeuwenburgh, New insights into the role of mitochondria in aging: mitochondrial dynamics and more, J. Cell Sci. 123 (2010) 2533–2542.
[40] A. Kowald, T.B. Kirkwood, The evolution and role of mitochondrial fusion and fission in aging and disease, Commun. Integr. Biol. 4 (2011) 627–629.
[41] J.L. Raucy, J.M. Lasker, C.S. Lieber, M. Black, Acetaminophen activation by human liver cytochromes P450IIE1 and P450IA2, Arch. Biochem. Biophys. 271 (1989) 270–283.
[42] X.M. Qi, L.L. Miao, Y. Cai, L.K. Gong, J. Ren, ROS generated by CYP450, especially CYP2E1, mediate mitochondrial dysfunction induced by tetrandrine in rat hepatocytes, Acta Pharmacol. Sin. 34 (2013) 1229–1236.
[43] E.N. Maldonado, J.J. Lemasters, ATP/ADP ratio, the missed connection between mitochondria and the Warburg effect, Mitochondrion 19 (2014) 78–84.
[44] A.V. Kuznetsov, R. Margreiter, A. Amberger, V. Saks, M. Grimm, Changes in mitochondrial redox state, membrane potential and calcium precede mitochondrial dysfunction in doxorubicin-induced cell death, Biochim. Biophys. Acta 1813 (2011) 1144–1152.
[45] I. Shokolenko, N. Venediktova, A. Bochkareva, G.L. Wilson, M.F. Alexeyev, Oxidative stress induces degradation of mitochondrial DNA, Nucleic Acids Res. 37 (2009) 2539–2548.
[46] H.P. Indo, M. Davidson, H.C. Yen, S. Suenaga, K. Tomita, T. Nishii, M. Higuchi, Y. Koga, T. Ozawa, H.J. Majima, Evidence of ROS generation by mitochondria in cells with impaired electron transport chain and mitochondrial DNA damage, Mitochondrion 7 (2007) 106–118.
[47] H. Tsutsui, S. Kinugawa, S. Matsushima, Oxidative stress and heart failure, Am. J. Physiol. Heart Circ. Physiol. 301 (2011) H2181–H2190.
[48] J. Zhang, P.A. Ney, Role of BNIP3 and NIX in cell death, autophagy, and mitophagy, Cell Death Differ. 16 (2009) 939–946.
[49] J.H. Lim, H.J. Lee, M. Ho Jung, J. Song, Coupling mitochondrial dysfunction to endoplasmic reticulum stress response: a molecular mechanism leading to hepatic insulin resistance, Cell. Signal. 21 (2009) 169–177.
[50] J.D. Malhotra, R.J. Kaufman, ER stress and its functional link to mitochondria: role in cell survival and death, Cold Spring Harb. Perspect. Biol. 3 (2011) a004424.